UNCERTAINTY ESTIMATION OF SIZE-OF-SOURCE EFFECT MEASUREMENT FOR 650 NM RADIATION THERMOMETERS

Fumihiro Sakuma, *Laina Ma*

National Institute of Advanced Industrial Science and Technology, Tsukuba, Japan, f-sakuma@aist.go.jp

Abstract − This paper describes the uncertainty estimation of the size-of-source effect (SSE) measurement for the standard radiation thermometers in the indirect method using an integrating sphere with a black spot as the source. We checked the agreement between two processes of changing the black spot size and changing the aperture size. The SSE contributions of each uncertainty factors were analyzed.

Keywords: size-of-source effect, radiation thermometer, uncertainty

1. INTRODUCTION

The size of source effect (SSE) is important in measuring by a radiation thermometer the temperature of a source with a different size from the calibration source. Three methods are available for the SSE measurement. They are a direct method, an indirect method [1] and a scanning method [2]. The direct method uses a large aperture blackbody whose aperture size can be changed. The indirect method uses an integrating sphere with a black spot in center and with an aperture. The scanning method moves the source or the thermometer sideway so that no large target is necessary in the measurement. It needs some calculation to obtain the SSE value. The indirect method has a merit that a small difference of two large signals is measured directly. This increases the signal to noise ratio. Therefore we employed the indirect method [3]. The review of the three methods are reported recently [4]. Many papers reported about SSE measurements using the indirect method [5, 6], however only one paper reported about the uncertainty of the indirect method [7]. It reported the case of large non-uniformity in radiance distribution. Here we report the uncertainty factors and their contribution.

2. INDIRECT METHOD

2.1. SSE definition

SSE is defined as the output increase of a radiation thermometer when the source size increases. Here we define SSE_{12} between two diameters d_1 and d_2 as follows.

$$SSE_{12} = \frac{V_2 - V_1}{V_2}, \tag{1}$$

or

$$V_2 = V_1 / (1 - SSE_{12}). \tag{2}$$

Here the output signals V_1 and V_2 refer to the diameters d_1 and d_2, respectively.

If we consider another diameter d_3, we obtain

$$\begin{aligned} SSE_{12} &= SSE_{13} + SSE_{32} - SSE_{13}SSE_{32} \\ &\approx SSE_{13} + SSE_{32} \end{aligned} \tag{3}$$

This approximation of the addition rule applies well because the SSE values are usually much smaller than 1. The subtraction law also applies.

$$SSE_{12} \approx SSE_{13} - SSE_{23}. \tag{4}$$

2.2. Integrating sphere and black spot

A large integrating sphere of 400 mm inner diameter with an exit port of 140 mm in diameter was used. The inside was coated with $BaSO_4$ paint. The sphere had six halogen lamps of 24 V 150 W around the port inside the sphere. The specifications of the sphere are given in Table 1. The sphere was on a computer-controlled stage of a 170 mm range in the horizontal direction and a 50 mm range in the vertical direction with a resolution of 10 μm.

Table 1 Specifications of large integrating sphere

Name	Large Integrating Sphere
Inner diameter	φ400 mm
Exit port diameter	φ140 mm
Inner wall	$BaSO_4$ coating
Lamps bulb cooling power source operation	Quartz-halogen lamp 24V 150W×6 Fan Stabilized direct current source for each lamp Constant voltage mode
Aperture	φ96, 72, 48, 36, 25, 18, 12, 9 or 6 mm
Black spot	φ1, 2, 3, 4, 5, 6, 9, 12, 16, 24 or 48 mm silk printed on quartz disk
Stage movement X range Z range resolution	Computer control ±85 mm ±25 mm 10 μm

Nine apertures from 6 mm to 96 mm in diameter and eleven quartz disks with silk-printed black spots of 1 mm to 48 mm in diameter were used. One aperture and one disk could be inserted at once in front of the exit port. A graphite blackbody cavity of a cone type with 6 mm in diameter and 11.2 mm in length was also used in the hole of a quartz disk to increase the reliability.

2.3. Radiation thermometer

Tests were performed on Topcon, Chino and LP3 0.65 μm radiation thermometers. Three radiation thermometers were made for a transfer standard and their qualities were much better than the commercial devices. Table 2 shows the specifications of three radiation thermometers.

Table 2: Radiation thermometer specifications.

Manufacturer	Topcon	Chino	KE
Type	OEP-PM-650NB	IR-RST 65H	LP3
Temperature range	900~3000 ºC	1000~3000 ºC	780~3500 ºC
Center Wavelength Band width	650 nm 15 nm	650 nm 13 nm	650 nm 10.5 nm
Measuring distance between objective lens and source	200 mm ~ ∞	400 mm ~ ∞	500 mm (440 mm with an extender) ~ 1050 mm
Objective focus distance	80 mm		140 mm
Aperture stop position	Between field stop and objective	Between field stop and objective	Between field stop and detector
Target size	0.5 mm at 250 mm distance	0.6 mm at 400 mm distance	0.5 mm at 400 mm distance
Resolution	0.1 K at 960 ºC	0.1 K at 1000 ºC	0.1 K at 923 ºC 0.02 K at 1423 ºC

2.4. Indirect method measurement

In the indirect method a radiation thermometer measures a black spot and a bright area whose outputs are V_b and V_r, respectively. V_r was measured in the half way between the black spot and the aperture. Data of a left halfway and a right one were measured and averaged. Because the V_r value was different for a different aperture or a different black spot, V_r was measured at each combination. In this case

$$V_b = V_2 - V_1, \qquad (5)$$

and

$$SSE_{12} = \frac{V_b}{V_r}. \qquad (6)$$

So V_r is used instead of V_2.

There are two processes to measure the SSE between two diameters, d_1 and d_2. One is the changing aperture process. It uses a black spot of d_1 diameter and an aperture of d_2 diameter. The diameter of d_2 is changed. This is a common method.

The other is the changing black spot process to use two black spots d_1 and d_2 and an aperture d_3. The SSE_{12} of the latter case was obtained by eq. (4).

This process is not reported anywhere. The process enables the measurement between two close diameters, 5 mm and 6 mm, for example. Some combinations can be measured by both processes. Therefore this process can check the reliability of the changing aperture process.

3. SSE DATA

Fig.1 shows the measured SSE data of a Topcon 0.65 μm radiation thermometer at a measuring distance of 490 mm. The reference diameter was 6 mm. This value was selected because the aperture diameter of our fixed-point blackbody was 6 mm. The changing aperture process is shown as a closed diamond and the changing black spot process is shown as an open diamond. Both processes agreed well with each other. The cavity data with the changing aperture process is shown as an open square. This also agrees with the data of the black spot (closed diamond).
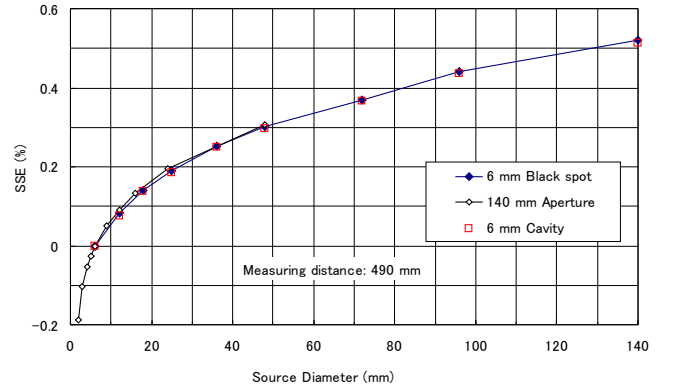

Fig. 1. SSE of a Topcon 0.65 μm radiation thermometer

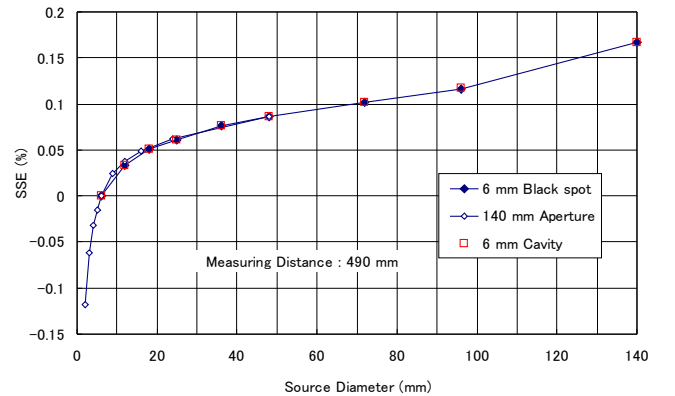Fig. 2. SSE of a Chino 0.65 μm radiation thermometer

Fig. 2 shows the measured SSE data of a Chino 0.65 μm radiation thermometer at a measuring distance of 490 mm. Compared to Fig. 1, the SSE of the Chino thermometer was about one third of the Topcon.

Fig. 3 shows the measured SSE data of an LP3 0.65 μm radiation thermometer at a measuring distance of 700 mm. The LP3's SSE was still better and about one tenth of the Topcon and one third of the Chino. The Objective lenses of the LP3 were changed to Apochromat. This change improved the SSE to half the value reported before [3]. Agreements between the changing black spot process and the changing aperture process were good. There was a small difference between the printed black spot data and the cavity data at apertures larger than the diameter of 96 mm.
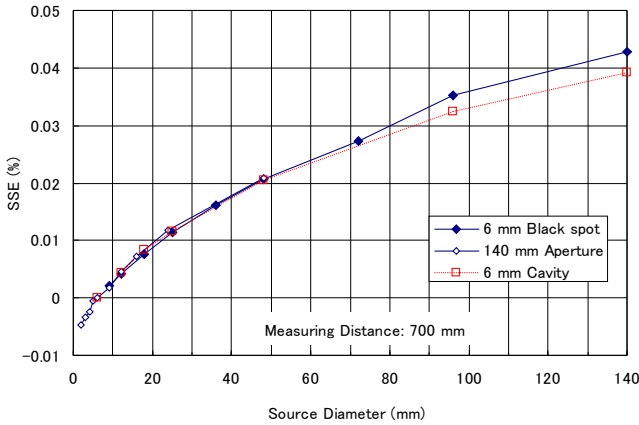

Fig. 3. SSE of an LP3 0.65 μm radiation thermometer

4. UNCERTAINTY FACTORS

Following factors were considered for the uncertainty of the SSE measurement.
reference black spot size d_1
aperture or black spot size d_2
black spot output V_b
bright area output V_r
measuring distance l_m
reproducibility

4.1. Black spot size

The black spots were silk-printed on a quartz glass. The specification of the size was ±0.1 mm. The contribution was expressed as follows.

$$u_{SSE}(d_1) = u(d_1)\frac{dSSE}{dd_1}. \qquad (7)$$

4.2. Aperture size

The apertures were made of aluminium disks and they were mechanically cut with a good precision. But it was painted with white barium sulphate in the back. The inner

diameter was smaller up to 0.3 mm due to the barium sulphate painting.

$$u_{SSE}(d_2) = u(d_2)\frac{dSSE}{dd_2}. \qquad (8)$$

The sensitivity factors in eqs. (7) and (8) were obtained from Figs. 1 to 3.

4.3. Black spot output

This measurement is very important because the output V_b is small and the sensitivity factor is large.

$$\frac{dSSE}{dV_b} = \frac{1}{V_r} = \frac{SSE}{V_b}. \qquad (9)$$

The output error for the black spot came from the transmittance and reflectance of the black spot. In the visible range the transmittance was usually negligibly small. The radiation from the source aperture was reflected by the objective lens to reach partly the black spot and then reflected back to the objective lens. If the measuring distance happened to be close to the diameter of the lens curvature and if the black spot surface is specular, this contribution can be significant. The initial black spot was specular and had some large reflectance in some cases, so we made an additional diffuse silk print on the black spot. Using a blackbody cavity for the black spot, we estimated this contribution by the difference between the black spot and the cavity.

4.4. Bright area output

The sensitivity factor is calculated as follows.

$$\frac{dSSE}{dV_r} = -\frac{V_b}{V_r^2} = -\frac{SSE}{V_r} \qquad (10)$$

Because V_r is large, the contribution is small. We consider following three cases.
radial non-uniformity of radiance
difference between left and right Radiance
difference between V_2 and V_r

A. Radial non-uniformity of radiance
Fig. 4 shows the radiance distribution at the 140 mm aperture of the integrating sphere measured in a 20-mm step by the Topcon 0.65 μm radiation thermometer. The center is the reference point and the difference is shown in %. The uniformity was good near the center but the spectral radiance decreased as it approached near the edge.

Fig. 5 shows the radiance dependence on the distance from the center. The four or eight data with the same distance were averaged and in the figure the diamond and the bar show the average and the standard deviation, respectively. The dependence was approximated by a quadratic equation shown by the solid line. The fitting was good. The decrease was about 0.3% at the edge. Because the thermometer used for the uniformity measurement had an SSE, the distribution difference was corrected for the SSE in Fig. 1. The broken line shows the corrected difference. The
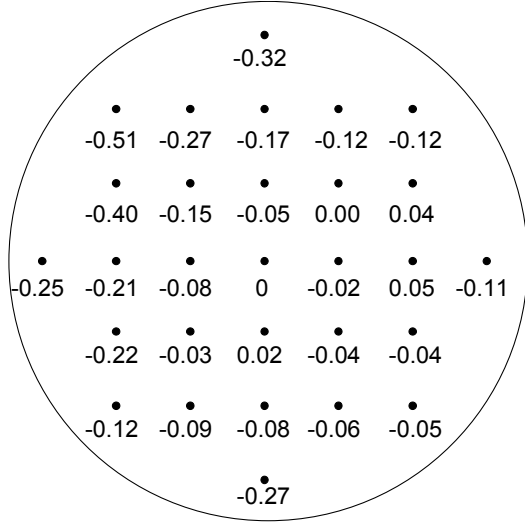
Fig. 4. Radiance non-uniformity of the sphere in %.

correction at the edge was about 0.1 %. By using the broken line, the output decrease of V_2 due to the distribution was estimated by using the following equation.

$$u_{SSE}{}^{Nu} = \int_{d_1}^{d_2} DW(s) \frac{dSSE}{ds} ds . \quad (11)$$

Here DW is the relative difference of radiance from the center. The contribution was calculated as 0.0002% at the edge for the Topcon thermometer.
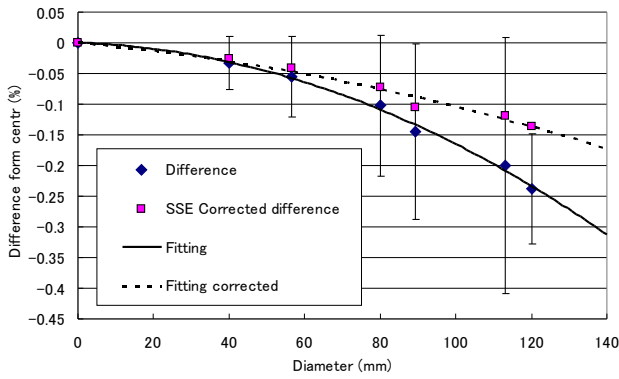

Fig. 5. Radiance dependence on the distance from center

B. Difference between left and right Radiance

In the SSE measurement we measured the left and right side halfway of the bright area and use the average of the outputs as V_r. The radiance difference between left and right was usually within 0.1 % and at most 0.2 %. A rectangular distribution was assumed.

C. Difference between V_2 and V_r

The SSE difference using V_r instead of V_2 was calculated by the following equation.

$$dSSE_{12} = \frac{V_b}{V_r} - \frac{V_b}{V_2} = SSE_{12} \cdot \frac{V_2 - V_r}{V_r} . \quad (12)$$

If the radiance distribution is uniform, following equation applies,

$$V_1 < V_r < V_2 . \quad (13)$$

From this we obtain

$$0 < \frac{V_2 - V_r}{V_r} < \frac{SSE_{12}}{1 - SSE_{12}} . \quad (14)$$

If we include the radiance distribution, we obtain following result of horizontal distribution from Fig. 4. Note that we used only halfway to the aperture and the average of the right and left sides was taken.

$$0 < \frac{V_2 - V_r}{V_r} < \frac{SSE_{12}}{1 - SSE_{12}} + 0.1\% . \quad (15)$$

4.5. Measuring distance

Fig. 6 shows the measuring distance dependence of the SSE of the 0.65 μm radiation thermometer. The data were measured at distances 25 cm, 49 cm, 70 cm and 100 cm. When the measuring distance was farther, the target area became larger and the solid angle of the source from the objective lens was smaller. These effects were small for the Topcon 0.65 μm radiation thermometer. We assumed an uncertainty of 10 mm in focus adjustment and alignment for Topcon and 15 mm for Chino and LP3.
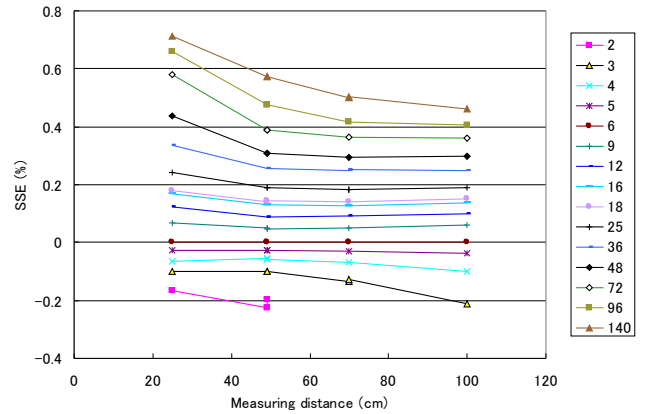

Fig. 6. Measuring distance dependence of SSE of the Topcon 0.65 μm radiation thermometer

4.6. Reproducibility

The reproducibility was obtained by five measurement of the SSE with changing the alignment. The reproducibility was 0.0006 % between 6 mm and 25 mm for Topcon. The focusing was very clear for the Topcon and LP3 thermometers but not clear for the Chino.

Table 3. Uncertainty budget for SSE measurement of a Topcon radiation thermometer using a printed black spot between 6 mm and 25 mm

Factor	u_i	Distribution factor	Sensitivity	u_{SSE}
Black spot size	0.1 mm	0.58	0.023 %/mm	0.0013 %
Aperture size	0.3 mm	1	0.0064 %/mm	0.0019 %
Output of black spot	0.0038 %	1	1	0.0038 %
Radial non-uniformity	0.00002 %	1	1	0.0000 %
Difference between left and right	0.2 %	0.58	0.002	0.0002 %
Difference between V_r and V_1	0.3 %	1	0.002	0.0005 %
Measring distance	10 mm	0.58	0.00013 %/mm	0.0008 %
Reproducibility	0.0006 %	1	1	0.0006 %
Combined standard uncertainty				0.0046 %

5. UNCERTAINTY RESULT

Table 3 shows the uncertainty budget for the SSE measurement of the Topcon 0.65 µm radiation thermometer between 6 mm and 25 mm diameters. The main factor was the measurement for the black spot output. This error was estimated from the output difference between the black spot and the blackbody cavity. Next main factor was the aperture size.

Fig. 7 shows the uncertainty in SSE measurement of the Topcon 0.65 µm radiation thermometer for various source diameters. For the source diameter larger than 10 mm the changing aperture process was used and otherwise the changing black spot process was used. Note that the abscissa was scaled in logarithm. Main uncertainty factors were the output of the black spot, the black spot size and the measuring distance. The black spot size contributed more for a smaller source diameter. In contrast, the measuring distance contributed more for a larger source diameter.
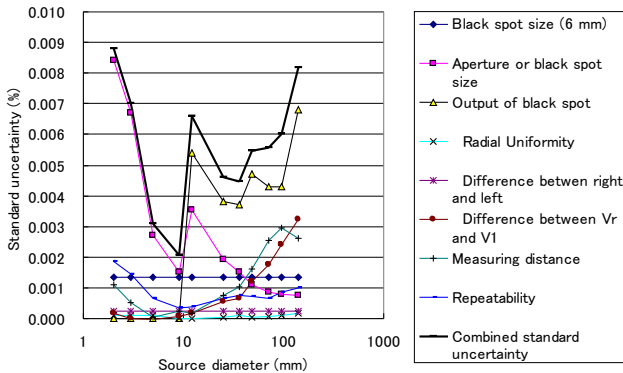

Fig. 7. Uncertainty in SSE measurement of the Topcon 0.65 µm radiation thermometer (k=1)

Fig. 8 shows the uncertainty in SSE measurement of the Chino 0.65 µm radiation thermometer. The main uncertainty factor was the black spot size and its contribution was larger at a smaller source diameter.

Fig. 9 shows the uncertainty in SSE measurement of the LP3 0.65 µm radiation thermometer. The main uncertainty factor was the output of the black spot. It contributed more at a larger source diameter. For the small source diameter the uncertainty was dominated by the repeatability. If we use a black body cavity for the black spot, we can neglect this factor and the standard uncertainty would be smaller than 0.001 %.
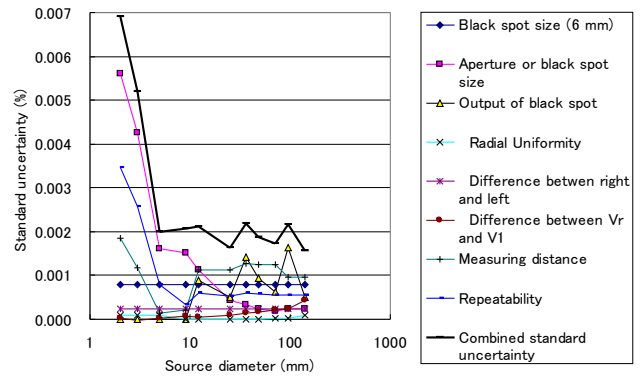

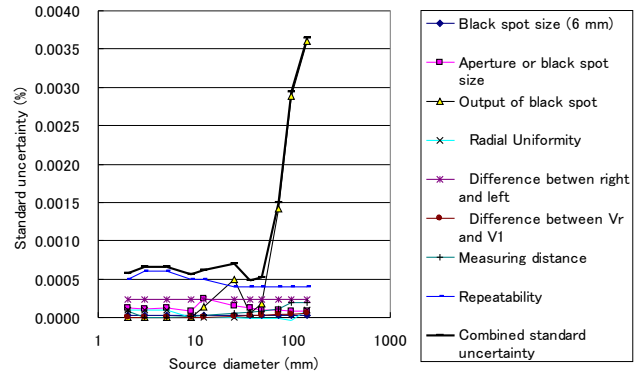Fig. 8. Uncertainty in SSE measurement of the Chino 0.65 µm radiation thermometer (k=1)

Fig. 9. Uncertainty in SSE measurement of the LP3 0.65 µm radiation thermometer (k=1)

6. CONCLUSIONS

The indirect method techniques for the SSE measurement at AIST were described, data of three 0.65 μm radiation thermometers were shown and their uncertainty factors were analyzed. The addition law for SSE was confirmed by changing both the aperture size and black spot size. The uncertainty of the SSE measurement depended on the thermometer. The standard uncertainties in the SSE measurement of the Topcon, Chino and LP3 thermometers were estimated as better than 0.01 %, 0.006 % and 0.004 %, respectively. If we use the blackbody cavity for the black spot, the standard uncertainty will become 0.001 % for the LP3.

ACKNOWLEDGMENTS

REFERENCES

[1] G. Machin, R. Sergienko, "A Comparative Study of Size-of-source-effect (SSE) Determination Techniques" *Proc. of TEMPMEKO* '01, Vol. 8, pp.155-160, 2001.

[2] M. Bart, E. W. M. van der Ham and P. Saunders "A New Method to Determine the Size-of-Source Effect" Int. J. Thermophys. Vol.28 2111–2117, 2007.

[3] F. Sakuma, L. Ma, Z. Yuan "Distance Effect and Size-of-source effect of Radiation Thermometers" *Proc. of TEMPMEKO* '01, Vol. 8, pp161-166, 2001.

[4] P. Saunders and H. Edgar "On the characterization and correction of the size-of-source effect in radiation thermometers" Metrologia Vol. 46 62–74, 2009.

[5] T. Ricolfi, L. Wang "Experiments and remarks on the size-of-source effect in precision radiation thermometry" *Proc. of TEMPMEKO* '93, Vol. 5, pp.161-165, 1993.

[6] H. W. Yoon, D. W. Allen, R. D. Saunders "Methods to reduce the size-of-source effect in radiation thermometers" *Proc. of TEMPMEKO* '04, Vol. 9, pp521-526, 2004.

[7] M. J. Martin, J. P. Perez, V. Chimenti, "An Alternative Calculation of the Size-of-source effect Uncertainty for Non-uniform Sources" I*nt. J. Thermophys*. Vol. 29 1131-1140, 2008.